FOKKER-PLANCK ANALYSIS OF TRANSVERSE COLLECTIVE INSTABILITIES IN ELECTRON STORAGE RINGS *

R. R. Lindberg, ANL, Argonne, IL 60439, USA

Abstract

We analyze single bunch transverse instabilities due to wakefields using a Fokker-Planck model. We expand on the work of Suzuki [1], writing out the linear matrix equation including chromaticity, both dipolar and quadrupolar transverse wakefields, and the effects of damping and diffusion due to the synchrotron radiation. The eigenvalues and eigenvectors determine the collective stability of the beam, and we show that the predicted threshold current for transverse instability and the profile of the unstable agree well with tracking simulations. In particular, we find that predicting collective stability for high energy electron beams at moderate to large values of chromaticity requires the full Fokker-Planck analysis to properly account for the effects of damping and diffusion due to synchrotron radiation.

INTRODUCTION

Understanding, predicting, and controlling collective instabilities is an imporatnt part of storage ring design and operation. Single bunch transverse instabilities are of particular importance in high-energy electron storage rings, as they typically set the limit on the maximum achievable current. The standard analysis of these instabilities decomposes the linearized Vlasov equation into normal modes, and then stability is determined by comparing the maximum growth rate with the transverse synchrotron and Landau damping rates (see, e.g., [2–6]). However, synchrotron emission results in both damping and diffusion in phase space, so that when synchrotron radiation provides the dominant damping mechanism it can render the Vlasov model incomplete. This is often the case for high energy electron storage rings, in which case a Fokker-Planck description must be employed to accurately predict stability. Here we build on the work of Ref. [1] to develop a more complete Fokker-Planck analysis of transverse stability, where particular attention is paid to the dynamics at large chromaticity.

MODEL EQUATIONS

Our starting point is very similar to the Hamiltonian models in the textbooks [4,5], but it includes the Fokker-Planck damping and diffusion associated with synchrotron radiation. Hence, the distribution function F obeys the equation

$$\frac{\partial F}{\partial s} + \{F, \mathcal{H}\} = \frac{2}{c\tau_z}\left[\sigma_\delta^2 \frac{\partial^2 F}{\partial p_z^2} + p_z \frac{\partial F}{\partial p_z} + F\right] + \frac{2}{c\tau_x}\left[\varepsilon_0 \mathcal{J}\frac{\partial^2 F}{\partial \mathcal{J}^2} + \frac{\varepsilon_0}{4\mathcal{J}}\frac{\partial^2 F}{\partial \Psi^2} + (\varepsilon_0 + \mathcal{J})\frac{\partial F}{\partial \mathcal{J}} + F\right]. \quad (1)$$

* Work supported by the U.S. Department of Energy, Office of Science, Office of Basic Energy Sciences, under Contract No. DE-AC02-06CH11357.

Here $(z, p_z) = (ct - s, -\delta)$ are the longitudinal variables, $(\mathcal{J}, \Psi)$ are the transverse action-angle variables, τ_z is the longitudinal damping time, σ_δ is the equilibrium energy spread, τ_x is the transverse damping time, ε_0 is the natural emittance, and $\{,\}$ denotes the Poisson bracket. We assume that the Hamiltonian $\mathcal{H}$ is comprised of the linear synchrotron and betatron motion, the first order chromaticity nonlinearity, and the lowest order effects of the dipolar wakefield. The basic procedure to simplify Eq. (1) is to

1. linearize with respect to perturbations about the self-consistent equilibrium;
2. assume that the transverse motion is described by dipole oscillations at the (chromaticity-corrected) betatron frequency
3. expand the longitudinal perturbation as a sum of linear modes in longitudinal action and angle;
4. solve the resulting eigenvalue problem to determine normal modes and complex frequencies as a function of current I and chromaticity ξ_x.

Mathematically, the first two steps can be expressed as

$$F = f_0(\mathcal{J})g_0(\mathcal{H}_z) + f_1(\Psi, \mathcal{J}; s)g_1(z, p_z; s), \quad (2)$$

where the equilibrium is a negative exponential in action,

$$f_0(\mathcal{J})g_0(\mathcal{H}_z) = \frac{e^{-\mathcal{J}/\varepsilon_0}}{2\pi\varepsilon_0}\frac{e^{-\mathcal{I}/\mathcal{I}}}{2\pi\langle\mathcal{I}\rangle}, \quad (3)$$

while the perturbation is a product of a simple dipole oscillation in the transverse dimension [2], with all the wakefield-driven complexity in the longitudinal perturbation g_1:

$$F_1 \propto -\sqrt{\mathcal{J}/2}f_0'(\mathcal{J})e^{-i[\Omega-(\Psi+k_\xi z)+\omega_\beta s/c]}g_1(z, p_z). \quad (4)$$

Here, $(\Psi + k_\xi z)$ represents the chromaticity corrected betatron oscillation phase, with the head-tail phase $k_\xi \equiv \omega_0\xi_x/\alpha_c c$ [7], while Ω is the complex frequency, and instability is characterized by $\Im(\Omega) > 0$.

We insert the perturbation (4) into the equation (1) and isolate the betatron oscillations by multiplying by $\sqrt{\mathcal{J}}e^{-i\Psi}$ and integrating over the transverse dimensions. When the dust clears the transverse part of the Fokker-Planck operator reduces to a simple damping term with damping time τ_x. This is because we have assumed that there is no interesting structure in the transverse plane; in contrast to this, we will find that the longitudinal Fokker-Planck damping and diffusion will depend on the longitudinal mode profile.

The next step is to linearize the problem for $|g_1| \ll 1$ and apply Sacherer's linear mode formalism by expanding g_1 as a sum of orthogonal linear modes

$$g_1(\Phi, r) = \sum_{q=0}^{\infty} \sum_{n=-q}^{\infty} a_q^n \frac{r^{n/2} L_q^n(r)}{\sqrt{(q+n)!/q!}} \frac{e^{-r}}{2\pi} e^{in\Phi}. \quad (5)$$

Here $L_q^n(r)$ is the associated Laguerre polynomial, the scaled longitudinal action $r \equiv \mathcal{I}/\langle \mathcal{I} \rangle$ with $\langle \mathcal{I} \rangle \equiv \sigma_z \sigma_\delta$, while the radial mode number is q and the azimuthal mode number is n; the number of nodes in r of the orthogonal mode functions equals p if $m \geq 0$, and $p+m$ if $0 > m \geq -p$. After a lengthy calculation similar to that in [4, 5] and detailed further in [8], we find that the linearized equation for the mode coefficient a_p^n becomes

$$\left[\frac{\Omega - m\omega_s}{c} + \frac{i}{c\tau_x} + \frac{i(2p+m)}{c\tau_z} \right] a_p^m + \frac{2\pi I}{\gamma I_A} \sum_{n,q} \mathsf{D}_{p,q}^{m,n} a_q^n = \frac{i}{2c\tau_z} \left(R_p^m a_{p+1}^{m-2} + T_p^m a_{p-1}^{m+2} \right), \quad (6)$$

where the Alfven current $I_A \approx 17$ kA and γ is the mean energy; the dipolar impedance coupling matrix is

$$\mathsf{D}_{p,q}^{m,n} = \frac{icI}{I_A} \frac{i^{m-n}}{\gamma Z_0} \int dk \; Z_D^\beta(k + k_\xi) e^{-k^2\sigma_z^2} \times \frac{(k\sigma_z/\sqrt{2})^{2p+m}}{\sqrt{p!(p+m)!}} \frac{(k\sigma_z/\sqrt{2})^{2q+n}}{\sqrt{q!(q+n)!}}, \quad (7)$$

while the Fokker-Planck diffusive coupling terms are

$$R_p^m = \sqrt{(p+1)(p+m)}, \quad T_p^m = \sqrt{p(p+m+1)}. \quad (8)$$

The first thing to note about the Fokker-Planck mode equation (6) is that the effective longitudinal damping time of the mode with radial, angular mode number (p, m) is $\tau_z/(2p+m)$. This decreasing damping time contrasts with the Vlasov results and was first found in Ref. [1]. It can be understood if we consider the fact that the diffusion time $t_{\rm diff}$ for a perturbation of scale length Δp_z is given by

$$t_{\rm diff} \sim \left(\frac{\Delta p_z}{\sigma_\delta} \right)^2 \tau_z \sim \frac{\tau_z}{2p+m}, \quad (9)$$

where the second scaling comes from the asymptotic properties of the Gauss-Laguerre functions. Hence, diffusion acts more strongly to smooth out the fine structure associated with high-order modes. It turns out that in the zero-chromaticity limit studied by Ref. [1] we have the usual transverse mode coupling instability (TMCI), wherein the $(p, m) = (0, 0)$ mode merges with the $(1, -1)$ mode. In this case the additional dissipative terms do not strongly affect the dynamics. On the other hand, increasing the chromaticity stabilizes the low-order modes such that the unstable profiles are comprised of a superposition of many higher-order modes. In this limit we will find that the increase in mode damping plays a significant role in stabilizing the dynamics.

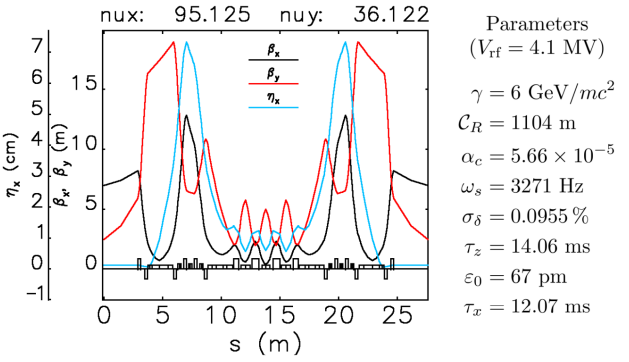

Figure 1: Twiss functions and basic parameters.

TRANSVERSE INSTABILITY FOR LARGE CHROMATICITY

We have found that the Fokker-Planck theory can be relatively well-approximated by retaining only the $(0, 0)$ and $(1, -1)$ modes provided the chromatic head-tail phase $k_\xi \sigma_z \lesssim 0.7$; in more familiar units this implies that $\xi \lesssim 0.7\alpha_c c/\omega_0 \sigma_z$, where α_c is the momentum compaction, ω_0 is the revolution frequency, and σ_z is the rms bunch length. At larger values of chromaticity many modes play a role in the dynamics, and the effectively large Fokker-Planck damping serves to help stabilize the dynamics.

To illustrate these effects, we have compared `elegant` [9] simulation results to our theory for a simplified model of the APS-U lattice [10] and its impedance [11]. In particular, we use the linear lattice and essential parameters of the 67 pm lattice shown in Fig. 1. The one simplification that we have made to the lattice is that we have artificially set the second order chromaticity to zero; it turns out that the large second order chromaticity lowers the instability thresholds in a manner that we have been able to incorporate in the model, but is beyond the scope of the present work.

In addition, for this study we have chosen to use the resistive wall impedance of the ring to model the transverse wakefields. Specifically, we assume that the chamber is either round or essentially flat with a half-gap of $b(s)$ that varies slowly over its length. Then, the ring-average dipole impedance can be approximated by

$$Z_D^\beta(k) = \eta_D \oint ds \; \beta_x(s) \frac{\mathrm{sgn}(k) - i}{\pi b(s)^3} \sqrt{\frac{Z_0 \rho(s)}{2|k|}}, \quad (10)$$

where $\rho(s)$ is the piece-wise constant resistivity, $\mathrm{sgn}(k)$ gives the sign of k, and the factor η_D depends on the chamber geometry, with $\eta_D = 1$ for round chambers and $\eta_D = \pi^2/24$ for flat chambers [12]. In summary, we take the scaled, β function-weighted dipolar impedance to be

$$Z_D^\beta(k) = Z_{\rm RW} \frac{\mathrm{sgn}(k) - i}{|k[1/\mathrm{m}]|^{1/2}} \quad \text{with} \quad Z_{\rm RW} = 25\ \mathrm{M\Omega}. \quad (11)$$

Finally, while the quadrupolar impedance vanishes in round vacuum chambers, the flat ID chambers have $Z_Q(k) = -Z_D(k)$; we discuss this effect in Ref. [8].

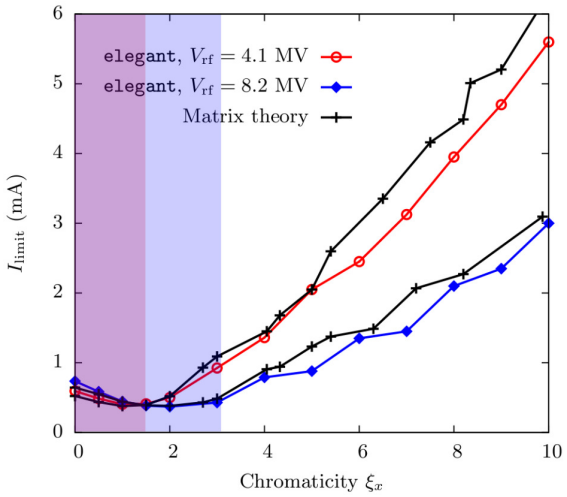

Figure 2: Comparison of theory and simulation for the predicted instability threshold as a function of chromaticity for the APS-U 67 pm lattice. The purple (blue) region shows where the 2-mode theory is valid for $V_{rf} = 4.1$ (8.2) MV.

We compare predictions for this model lattice and impedance in Fig. 2, where we plot the instability threshold current I_{thresh} as a function of chromaticity for both the Fokker-Planck theory and the `elegant` simulations. We see that the theory and simulation agrees well over a wide range of chromaticity at both the nominal voltage of $V_{rf} = 4.1$ MV and the hypothetical $V_{rf} = 8.2$ MV.

At vanishing chromaticity we have the usual TMCI, where the impedance shifts the frequency of the $m = 0$ mode until it merges with the (nearly constant) $m = -1$ mode frequency $\approx \omega_s$. In this case the threshold current increases as the frequency difference $\sim \omega_s$ increases, so that increasing the rf voltage leads to larger I_{thresh}. As mentioned earlier the two-mode approximation is valid if the chromaticity "low"; we show this region defined by $k_\xi \sigma_z < 0.7$ by the purple (blue) shaded region for an rf voltage of 4.1 (8.2) MV in Fig. 2. In this region it turns out that increasing the chromaticity first decreases I_{thresh} as the dipolar matrix becomes complex, and then increases the current as the mode merging picture becomes a less accurate description of how the instability develops. Finally, the edge of the shaded region shows where the two mode approximation predicts no instability, so that accurate madeling must incorporate more higher order modes.

As the chromaticity is increased further, different spectral regions of the impedance play a role according to the head-tail frequency shift. In addition, the unstable mode profile becomes a superposition of an ever increasing number of orthogonal modes. We show a comparison between the unstable mode profile predicted by theory and extracted from the `elegant` simulations at $\xi = 5$ in Fig. 3. Figure 3 shows that the unstable mode is largely comprised of $m = -4$ modes, although roughly 20% have $m = -3$ and $m = -5$. For these parameters Landau damping plays a negligible role in determining stability.

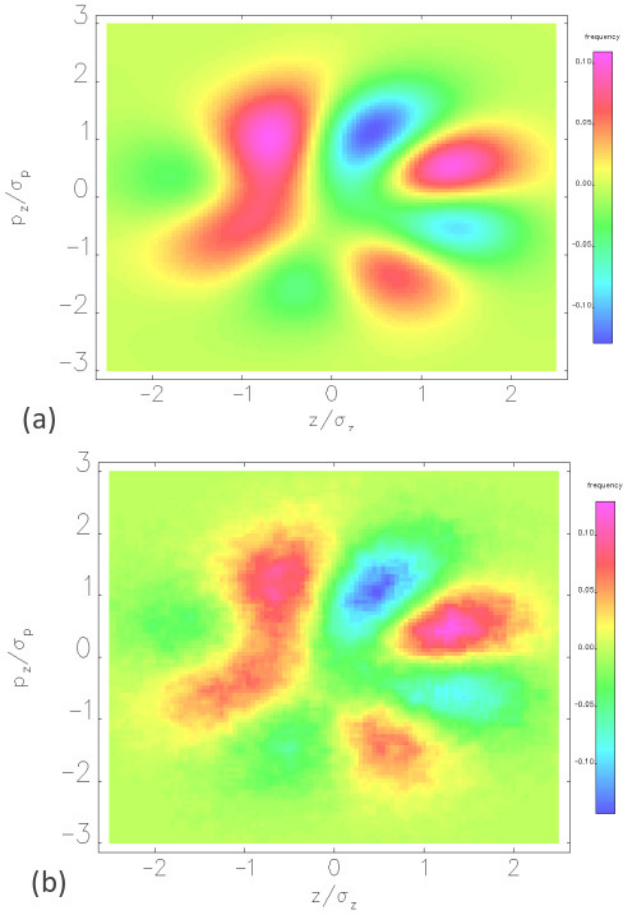

Figure 3: Comparison of theory (a) with simulation (b) for $\Im(g_1)$ of the unstable mode at $\xi = 5$ and $I = 2.25$ mA.

CONCLUSIONS

We have presented a Fokker-Planck theory of collective instability, and shown that it agrees well with simulation for a model problem. We have found that the classic TMCI picture holds for only a limited range about $\xi = 0$. For most of the considered range of chromaticity the unstable eigenmode is comprised of many basis modes, and longer bunch lengths with lower peak currents lead to higher instability thresholds. We believe that similar analysis should apply to other high energy electron storage rings, although the analysis becomes complicated when the longitudinal potential is distorted by wakefields and/or higher harmonic rf systems.

REFERENCES

[1] T. Suzuki. *Particle Accel*, 20:79 (1986).

[2] F. Sacherer. Report 72-5, CERN/SI-BR (1972).

[3] F. Sacherer. Report 76-21, CERN/PS-BR (1976).

[4] A. W. Chao. *Physics of Collective Beam Instabilities in High Energy Accelerators*. Wiley, New York (1993).

[5] K. Y. Ng. *Physics of Intensity Dependent Beam Instabilities*. World Scientific, Singapore (2006).

[6] A. Burov. *Phys Rev ST Accel Beams*, 17:021007 (2014).

[7] M. Sands. Report 121, SLAC (1970).

[8] R. R. Lindberg. Submitted to *Phys. Rev. ST Accel. Beams*.

[9] M. Borland. ANL/APS LS-287, Advanced Photon Source (2000).

[10] M. Borland et al. *Proc. IPAC15*, 1776–1779 (2015).

[11] R. R. Lindberg et al. *IPAC15*, 1825–1827 (2015).

[12] L. J. Laslett et al. *Rev Sci Instrum*, 36:436 (1965).